Unconventional Imaging with Contained Granular Media*

Marco B. Quadrelli†, Scott Basinger[a], Erkin Sidick[a]
[a]Jet Propulsion Laboratory, California Institute of Technology, 4800 Oak Grove Drive, Pasadena, CA, 91109-8099

ABSTRACT

Typically, the cost of a space-borne imaging system is driven by the size and mass of the primary aperture. The solution that we propose uses a method to construct an imaging system in space in which the nonlinear optical properties of a cloud of micron-sized particles, shaped into a specific surface by electromagnetic means, and allows one to form a very large and lightweight aperture of an optical system, hence reducing overall mass and cost. Recent work at JPL has investigated the feasibility of a granular imaging system, concluding that such a system could be built and controlled in orbit. We conducted experiments and simulation of the optical response of a granular lens. In all cases, the optical response, measured by the Modulation Transfer Function, of hexagonal reflectors was closely comparable to that of a conventional spherical mirror. We conducted some further analyses by evaluating the sensitivity to fill factor and grain shape, and found a marked sensitivity to fill factor but no sensitivity to grain shape. We have also found that at fill factors as low as 30%, the reflection from a granular lens is still excellent. Furthermore, we replaced the monolithic primary mirror in an existing integrated model of an optical system (WFIRST Coronagraph) with a granular lens, and found that the granular lens that can be useful for exoplanet detection provides excellent contrast levels. We will present our testbed and simulation results in this paper.

Keywords: unconventional imaging, space telescopes, granular medium, trapping, confinement

1. INTRODUCTION

Typically, the cost of an optical system is driven by the size and mass of the primary aperture [1]. We propose large, lightweight, imaging systems based on a granular medium layer held together and manipulated remotely by laser light pressure and EM radiation. Inspired by the light scattering and focusing properties of distributed optical assemblies in nature, such as rainbows and aerosols [9,11,14], and by recent laboratory successes in optical trapping and manipulation [2,3,4,10,12,32,33], we propose a unique combination of space optics and autonomous robotic system technology, to enable a new vision of space system architecture with applications to ultra-lightweight space optics. We call this system the Granular Imager (GI), and refer to it as aerosol lens, granular telescope, or contained diffused optical medium.

Recent work [24,25,26,27,28,29] has investigated the feasibility of a granular imaging system, concluding that such a system could be built and controlled in orbit, and could be used effectively as an imaging system in the radar and visible bands. In our initial effort, focused on the astrophysical and radar tomography applications of the Granular Imager, we have: a) gained initial insight into the physics of granular systems in space; b) developed an approach to trap and align a cloud of reflective particles; c) designed optical imaging systems that include multistage wavefront control to compensate for uncorrectable errors due to the stochastic nature of the cloud; d) identified multi-frame blind deconvolution algorithms that reconstruct image estimates from an ensemble of incoherent images; e) developed electromagnetic models to study the granular medium reflective and transmissive response in the microwave band; and f) developed a preliminary multi-scale simulation, which predicts the time evolution of the imaging system kept in formation as it orbits the Earth.

This new concept is based on recent understandings in the physics of optical manipulation of small particles in the laboratory and the engineering of distributed ensembles of spacecraft swarms to shape an orbiting cloud of micron-sized objects. The parameter space of the Granular Imager includes distributes spacecraft, multi-functional materials, large apertures smart materials, system autonomy, and interaction with the space environment. We believe that

† corresponding author, Research Technologist and Group Lead, Mail Stop 198-219, Autonomous Systems Division, Jet Propulsion Laboratory, California Institute of Technology, 4800 Oak Grove Drive, Pasadena, CA 91109-8099, marco.b.quadrelli@jpl.nasa.gov

thoroughly understanding and leveraging this parameter space will enable new large-scale NASA mission applications [6,7] and develop new technology in the areas of Astrophysical Imaging Systems and Remote Sensing because the cloud can operate as an adaptive optical imaging sensor. Figure 1 depicts the concept behind the Granular Imager: a trapped cloud of reflective grains operates as a mirror. While achieving the feasibility of constructing one single aperture out of the cloud is the main topic of this work, it is clear that multiple orbiting aerosol lenses could also combine their power to synthesize a much larger aperture in space to enable challenging goals such as exo-planet detection. Furthermore, this effort could establish feasibility of key issues related to material properties, remote manipulation, and autonomy characteristics of cloud in orbit. There are several types of endeavors (science missions) that could be enabled by this type of approach, i.e. it can enable new astrophysical imaging systems, exo-planet search, large apertures allow for unprecedented high resolution to discern continents and important features of other planets, hyperspectral imaging, adaptive systems, spectroscopy imaging through limb, and stable optical systems from Lagrange-points. Furthermore, future micro-miniaturization might hold promise of a further extension of our dust aperture concept to other more exciting smart dust concepts with other associated capabilities. Figure 1 depicts the evolution of large space observatories, indicating that solutions with very low area to mass ratio are highly desirable.

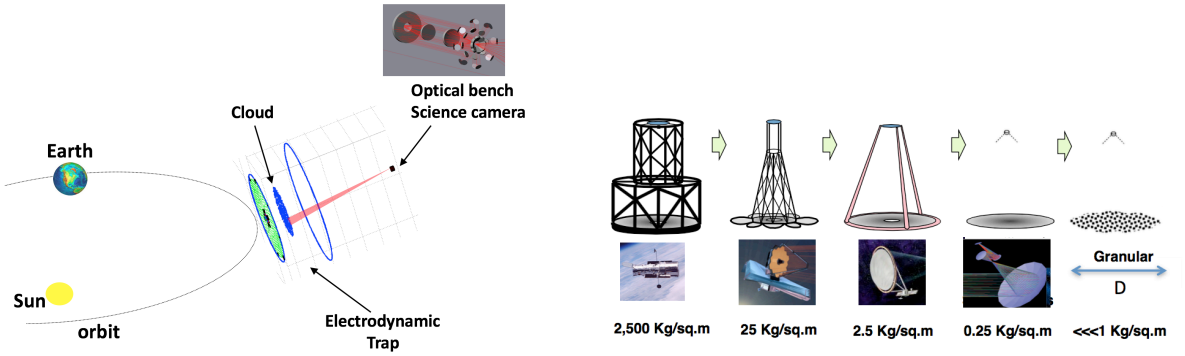

Figure 1. (Left) The Granular Imager: a trapped cloud of reflective grains operates as a mirror. (Right) Evolution of large space telescopes.

The Granular Imager addresses challenges for development of: a) new autonomous systems, as it may open the door to innovative applications of formation flying and autonomy technology in space; b) novel approaches to large precision imaging systems; and c) innovative applications of granular media as multi-scale, multi-physics, multi-functional systems. We have assessed the basic elements of granular imaging systems in the context of two relevant mission scenarios: an astrophysical imager and a radar mapper. From a science perspective, the granular imager concept will open new frontiers of exploration and scientific discovery in space science. From a robotic system perspective, we have studied autonomy solutions and multiscale behavior of complex aerospace systems. From the materials perspective, we have explored a novel use of granular media in space.

Section 2 answers the question "How does it work?. Section 3 discusses the system configuration and cost. Section 4 addresses the potential applications for astrophysics. Section 5 describes the sensing and control challenges. Section 6 discusses recent work on the modeling and experiments of the interaction of the incident waavefront with the granular medium. Section 7 concludes the paper.

2. HOW DOES IT WORK?

The paradigm that makes this granular imager possible is based on: a) avoiding any physical structure and sensing/actuation hardware on the primary aperture, thus lowering the system cost (driven by the mass and complexity of the primary); b) using at-a-distance trapping and manipulation to confine and shape the cloud acting as primary aperture; and c) relaxing the optical figure control requirements by doing the best possible job in software with state-of-the-art computational imaging algorithms. Granular matter is considered to be the 5th state of matter (after solid, liquid,

gaseous, and plasma) by virtue of its peculiar response characteristics (cohesiveness, fluid behavior, compactification, phase transformation capability, and other properties [11]). However, the dynamics, controllable properties, and consequent benefits of engineering and manipulating granular matter, such as dust grains, powders, and aerosols, is poorly known to the space exploration community. This research leverages the expertise developed in autonomous space systems technology at NASA/JPL (specifically, formation flying for astrophysical imaging [20]); adaptive optics of astrophysical spaceborne observatories, such as the Spitzer Space Telescope, SIM Planetquest, Terrestrial Planetfinder, and the James Webb Space Telescope [1,15,16,17,19] or the Eyeglass telescope [13]; and recent achievements in optical manipulation at Rochester Institute of Technology on radiation pressure force and torque [36], to investigate the possibility of deploying, focusing, retargeting the cloud in space, and adding autonomy to the cloud of particles in order to produce an adaptive optics light collector. As background, A.J. Palmer [22,23], proposed to use an aerosol of dielectric particles as a holographic lens. Labeyrie's pellicle telescope [15,16,17] was the inspiration for a prior NIAC study [19]. More recently, the optical trapping of aerosols at the micro-scale has been demonstrated in the laboratory [9,18,35]. Our concept is to enable the large-scale electromagnetic utilization of an active cloud of incoherent matter. Recent and rapid advances in the optical manipulation area have the potential to revolutionize micro- and nano-manipulation of objects in much the same way that the discovery of optical tweezers, now routinely used for DNA manipulation, did 40 years ago. Although the radiation pressure force on a macroscopic body is weak, a few milliwatts of laser power are sufficient to achieve a force in the pico-newton range. There is also another major advantage. For some NASA applications, the synthesis of large apertures made of large numbers of emitters/receivers placed with structural disorder is desirable. For a disordered cloud, focusing of light from an object is achieved by modulating the phase of the distributed radiators so as to obtain a conic phase surface; it was observed that by randomizing the emitter positions, the beam achieves better quality [3,4,39]. The ideal system is a cloud of spatially disordered dust-like objects that can be optically manipulated: it is highly reconfigurable, fault-tolerant, self-healing, and scalable to very large aperture sizes at low cost. The solution that we propose is to construct a distributed imaging system in space in which the primary element is a cloud of micron-sized engineered particles, shaped along a specific surface by light pressure, allowing it to form a very large and lightweight aperture of an imaging system, hence reducing overall mass and cost. A cloud of spatially disordered dusk-like objects can be optically manipulated to be highly reconfigurable, self-healing, and fault-tolerant to allow very large aperture sizes at low cost. The optical system can have a variable focal length, combined reflective and refractive lens designs, and hyperspectral imaging capabilities.

The imaging through retargeting and realization of boresight and wavefront control of an orbiting cloud represent a rich area of investigation, independently of the applications because of the multiple spatial and temporal scales involved to enable an integrated mission design in astrophysical imaging, exoplanet search, large aperture that allows unprecedented high resolution, and hyperspectral imaging, and spectroscopy, as well as novel radar imaging concepts. In a past study on the laser-trapped mirror [19], a main challenge identified by the investigators was related to cloud overheating from a focused beam. Since most of the optical manipulation experiments are done on Earth in water or air, there is natural heat dissipation into a conductive medium. In space, there is no intervening medium (except for the tenuous space plasma, which provides less heat dissipation than air or water), hence cooling in optical binding experiments cannot be achieved. Although those earlier experiments achieved small-scale coherent structures in a constrained two-dimensional aqueous chamber using spherical particles, large-scale three-dimensional structures composed of optically functional particles in a space environment presented untested challenges. In our study, we avoid tightly focused beams, opting instead to gently nudge the particles using combinations of radiation pressure and electromagnetic torque induced by polarizing the beam with relatively low irradiance, thereby minimizing the source of heat. Furthermore, we engineer the particles to radiate heat and optimize their response to the applied fields. For example, each grain has a tail that may be aligned to the polarization direction of a laser beam, thereby achieving a coherent alignment of all the exposed particles. Optical binding required weakly interacting spherical particles over a short range. In contrast, our approach assumes non-interacting, arbitrarily shaped particles that may be widely spaced. Compared to conventional large aperture systems, our proposed concept is unique in that: a) it would be a structure-less, very lightweight system, leading to areal densities of 0.1 kg/m2 or less, compared to 10 kg/m2 or more of monolithic apertures; b) one cloud could combine with other clouds to form extremely large apertures; c) would be easy to package, not requiring structural elements; d) line-of-sight retargeting and figure control would be realized remotely using electromagnetic fields, without the need for complex sensors and actuators on the backing structure. These properties enable new mission architectures, and are in contrast to current state-of-the-art systems which are limited to much smaller sizes and are quite massive. The paradigm that makes this granular imager possible is based on: a) avoiding any physical structure and sensing/actuation hardware on the primary aperture; b) using at-a-distance trapping and manipulation to confine and shape the cloud acting as primary; and c) relaxing the optical figure control requirements

via state-of-the-art computational imaging algorithms. Table 1 compares the Granular Imager to existing telescope technologies.

Table 1. State of the art of current telescope technology.

Metric	Conventional Mirror SoA	Light-Weight Mirror SoA	Inflatable	Liquid mirror	Granular Imager
Mass Areal Density	40-100 kg/m2	10-20 kg/m2	<5 kg/m2	100-200 kg/m2	<<0.1 kg/m2
Surface Figure Error	10 nm RMS	14 nm RMS	<5 micro-m RMS	<5 micro-m RMS	<100 nm RMS
Surface microroughness	<5Å	<10Å	500 nm	20 nm	< 100Å
First free-free mode	>100Hz	>100Hz	>1 Hz	>10 Hz	< 1 mHz
Size	0.1 to 2.4m and larger	0.3 to 1.35m and larger	1 to 10 m	1 to 10 m	> 10 m
Deployable	No	No	Yes	No	Yes
Thermal stability	Low CTE	Thermally controlled	Thermally Controlled	Thermally Controlled	Thermally Controlled
Formation Flying	No	No	No	No	Yes
Wavelength	Visible	Visible	Visible/Radar	Visible	Visible/Radar
Orbit	L2	L2	LEO	Ground	GEO/L2
Backing Structure	Yes	Yes	Yes	Yes	No
Packaging	Complex	Complex	Medium	N/A	Simple
Retargeting	RCS	RCS	RCS	No	Optical/EM
Fault-tolerance	Low	Low	Low	Low	High

Key technologies that were relevant to mature the concept are discussed next. Granular imaging systems will require complex multistage control methodologies and diffractive optics techniques. To achieve this goal, the Phase II multiscale system simulation of the science campaign was essential to assess system-level performance for representative scenarios. Also, system-level integrated modeling and simulation of reflective, refractive, and diffractive configurations in different frequency bands is essential to flow down requirements. Speckle imaging experiments are essential to demonstrate that optical imaging based on spatial disorder is practical, and we have begun experimenting with computational optics techniques to retrieve the image in the presence of noise [5,17,30,31,37,40]. Optical cooling experiments are essential to demonstrate the multiple levels of precision in trapping and containment of the granular aperture. Recent work based on the optical vortex [32] expands optical manipulation of particles into a gas media and provides full control over trapped particles, including the optical transport and pinpoint positioning of 100 micron objects over a meter-scale distance with 10 micron accuracy. Finally, a cost-benefit analysis is essential to make the cloud aperture more promising compared to a monolithic aperture. The key feasibility issues related to cost are system testing and system integration. In this regard, the in-depth study of reflective, refractive, and diffractive systems will provide a unique approach to flow down imaging requirements down to the cloud level. The key feasibility issues related to system performance are analyzing whether there is sufficient sensing and control authority to ensure a stable wavefront through the granular medium. In this regard, we will also explore imaging architectures in a less demanding frequency band (i.e., radar), thus accelerating the maturation at the system level. The key feasibility issues related to risk are providing sufficient system verification and validation, and the development of a multiscale system simulation will make requirement verification possible. The key feasibility issues related to system development time are sufficient maturity of the cooling and speckle imaging experiments. Successful cooling experiments (critical technology) would enable the demonstration of the concept feasibility in a ground laboratory, and successfully accomplishing these experiments would contribute to raising the system TRL significantly.

Promising developments in the optics of disordered media have been carried out recently. In [38], scattering in a medium behind a lens was used to improve the focusing resolution to beyond the diffraction limit of that lens. The authors found that, surprisingly, the shape of the focus is not affected by experimental limitations of the wavefront modulator: the focus is always exactly as sharp as is theoretically possible. Disordered scattering has been applied to improve resolution and bandwidth in imaging and communication with ultrasound, radio waves and microwaves [8,32], and significant sub-wavelength effects have been demonstrated. The results in [8] were the first demonstration that similar resolution improvements can be obtained in photonics. Calculations [10] indicate that useful optical superresolution can also be achieved using disordered plasmonic nanostructures. In [8], the authors demonstrated that turbidity both improves the spatial resolution of an objective lens beyond its diffraction limit and extends its field of

view. This is called Turbid Lens Imaging (TLI). These two improvements result from the angular and spatial spread of light by multiple scatterings in a disordered medium. The development of TLI to exploit multiple scattering allows a turbid medium to become a unique lens with counterintuitive imaging properties. This work is an important step beyond previous studies that used a turbid medium to achieve subdiffraction focusing in ultrasound and optics and near-field focusing with microwaves [Choi]. Our work uses turbid media to achieve subdiffraction imaging, not focusing. We open a way to convert a random medium into a superlens with no need of any metamaterial by using the fact that disordered media with structures finer than a wavelength can capture evanescent waves.

The design concept of the Granular Imager follows a top-down approach. At the large-scale, the imaging system, including the detector, is held in shape by means of formation flying technology [3,20], i.e. using precision metrology and precision thrusters to achieve a "virtual truss". At this scale, the granular cloud forming the primary aperture can then be thought of behaving as an equivalent rigid object. Established wave front sensing and control techniques of adaptive optics are then used to stabilize the image assuming the granular aperture behaves as an equivalent monolithic aperture. We then invoke methods of sparse aperture technology, such as Golay arrays [31], to precisely formation-fly many clouds, which, at the microscale, are spatially random, but at the macroscale form a regular array. Through optical manipulation technology, we sense and control the average alignment of the grains within each cloud to provide a cloud figure shape that is adequate for our goals. Therefore, the top-down formation flying and adaptive optics approach merges with the bottom-up optical manipulation approach to achieve our goal.

Earnshaw's theorem ([9]) states that a body with mass, static charges, magnetization, or currents, in a steady electric, magnetic, or gravity field cannot be maintained in stable equilibrium under the influence of electric, magnetic, or gravitational forces alone. The consequence of this theorem is that a static (electric, magnetic, gravitational) system of (charges, current, inertia) carrying structures has at least one unstable mode of deformation in the absence of mechanical constraints (i.e., mass must not be free) and feedback control currents (or moving masses providing restoring forces). We circumvent this theorem by the addition of the buffer gas, which provides additional dissipation, and by feeding back images of the cloud to the boundary electrodes so that a stable Coulomb crystal can be achieved. The stable confinement and rigidization of the cloud is then sequentially obtained as follows. First, the diffuse reflective medium is dispensed within a transparent inflatable envelope containing a neutral buffer gas, such as Ar. The released cloud is then guided into a stable Coulomb crystal by adjusting the boundary potentials of an electrodynamic trap to satisfy the condition for crystal formation.

3. SYSTEM CONFIGURATION AND COST

An electrodynamic trap of the double-ring type is shown in the GI configuration in Figure 3. Once the crystal has been formed, the rotational alignment of the grains into the incoming wavefront is achieved by rastering a laser beam across the extent of the cloud. The radiation pressure of the laser beam rotates the grains in the proper direction.

A typical orbital scenario would follow these steps: (1) the cloud is first released; 2) it is electromagnetically trapped to avoid dissipation and disruption by gravitational forces and shaped into a two-dimensional object (coarse figure control); and 3) the grains could be aligned to the incoming wavefront by means of rastering laser beams (fine figure control) leading to a surface with acceptable imaging characteristics, i.e. the primary aperture. By modulating the spatial and temporal distribution of the confining fields, the cloud can be retargeted as desired. The secondary would be in formation flight with the primary aperture. Established computational imaging techniques would process the sequence of images to remove additional noise (scattering, speckle) and further improve the image quality. Beam shaping of a cloud of particles is possible by molding the cloud with the gradient force, say in the x-y plane, and by further molding the cloud in the z-direction by the combined optical scattering force and gravitational forces arising from the orbital dynamics (tidal forces).

An important element of the design is the consideration of the interaction with the space environment. Small grains can be dielectric, or not conducting, but they will charge negative when in equilibrium with local plasma (and shadowed), due to continuous bombardment from electrons—the ambient electron current typically exceeds the proton current as the electrons, for roughly the same thermal energy, have significantly higher velocities. Once illuminated by Sun, UV radiation will cause photoemission, equilibrium potential will be offset, and grains will become positively charged, hence disrupting equilibrium. Continuous electromagnetic trapping becomes necessary in the solar wind as the solar plasma will entrain the charged dust (e.g., a comet's plasma tail)—a sun-shade might alleviate the problem or

enveloping the cloud inside a balloon (inflatable). Continuous solar wind and radiation pressure exposure in L2 could complicate particle containment. Therefore, within the Earth's magnetosphere at GEO, we need to expect additional political problems associated with possible space debris generation and associated impact on expensive assets. Also, the Debye length is large, grains can interact with each other, which will not preclude clustering of grains, like West Ford needles. Conversely, outside of magnetosphere, in the Sun-Earth L2 point, the Debye length is moderate, grains will still interact with each other. The dynamics will be dominated by solar wind, from 400 km/s when Sun quiescent and up to 3000 km/s during CME. Hence grains might be entrapped easily by the solar wind. In this regime, it will need continuous confinement mechanism, or balloon containment. Plasma PIC (particle-in-cell) simulations are needed to show cloud stability in space environment, under different space environment and trapping mechanisms. Figure 2 shows a prototype configuration for 10 meter Granular Imager with electromagnetic confinement rings: the set of two rings in the lower part of the figure represents a double-ring electromagnetic confinement system, and the cylinder above represents the adaptive optics stage, with science camera. The top inflatable ring is empty inside, while the bottom inflatable ring is a torus which keeps the membrane with the electrode patches taut. The granular aperture is trapped in the space between the two electrode systems. Figures 3 also shows the configuration of the Granular Imager where the granular medium is kept floated inside an inflatable envelope, filled with a buffer gas such as Argon. The need for this confinement inside an inflatable envelope originates in the need to mitigate the orbital debris generation problem. Figure 4 shows details of the inflatable canopy. Figure 4 also depicts the mechanism of retargeting of the granular cloud inside inflatable canopy.

The total system cost was calculated based on existing cost models available in literature (NASA Advanced Mission Cost Model [34]). This cost determination was based on the assumptions of technology maturation in Table 2, the subsystem masses in Table 3, and the Design Reference Mission DRM-2 in Table 4. If N is the number of aerosol clouds, M the total mass, λ the wavelength, the dollar amount is in billion, and we introduce difficulty levels DL as: -2=very low, -1=low, 0=average, 1=high, and 2=very high, the cost model is written as:

$$Cost = \$2.25 \times (M/10{,}000kg)^{0.654} \times 1.555^{DL} \times N^{-0.406} \times \lambda^{-0.5} \quad (1)$$

Table 5 summarizes the driving requirements and needed technologies for Granular Imager, and substantiate the difficulty level considered in the cost evaluation. We assumed 10^7 grains per aerosol patch, a grain density of 2500 kg/m^3, 3 patches of diameter 1 meter, difficulty level 2, cloud thickness 1 micron. Figure 5 shows the results of these computations for a wavelength of 0.3 micron, i.e. the effective aperture mass and imaging system cost vs. effective diameter, for monolithic and cloud apertures, demonstrating the enormous cost reduction for the orbiting cloud, compared to a monolithic system. This cost model, however, does not include the cost of the laser manipulation system, or the impact of utilizing a system in formation flight, only the cost of the equivalent aperture compared to a monolithic aperture.

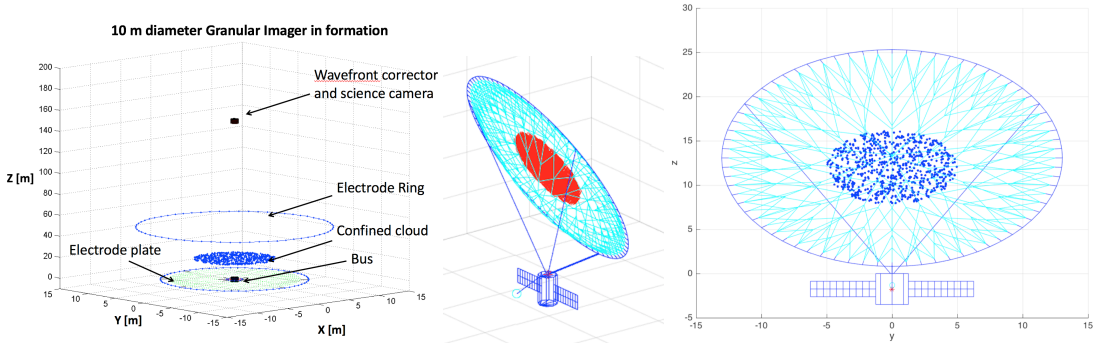

Figure 2. Prototype configuration for 10 meter Granular Imager with electromagnetic confinement rings (left), and immersed in a buffer gas inside an inflatable envelope (center, right).

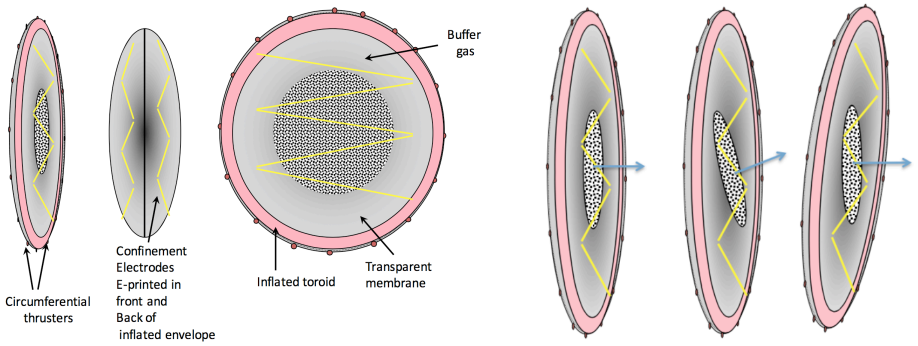

Figure 3. Details of granular medium inside inflatable aperture (left), options for cloud boresight redirection by beam steering of electrode potentials (right). Confining electrodes (yellow) are printed on inflatable membrane.

Table 2. System Configuration and perceived TRL.

Element	Comments	Perceived TRL
Imager configuration	Formation flying telescope, from NASA TA	**2-3**
Science	Exoplanet detection, coronography, synthetic aperture radar imager, tested on ground	**8**
Adaptive optics	Multistage WFSC, tested on Keck telescope	**6**
Imaging technology	Computational imaging	**3-4**
Radar imaging technology	Radar ultra-wideband imaging. Many systems flown. Reflector technology at low TRL.	**3-4 (reflector) 9 (system**
Primary (Cloud) deployment and maintenance	Electrodynamic confinement, laser trapping developed at component level. Cloud containment and maintenance maneuvers would be done periodically once the system has been deployed.	**6-7 (component) 2 (system)**
Grains	Microfabricated, deployed from sublimating drum	**5-6**
Orbit	GEO (many telecomm satellites) or Sun-Earth L2 (Herschel, Planck)	**9**
Payload size	1m patch, scalable	**2**
Conops	In all phases the cloud is stabilized. All sensors/actuators, control loops, comm., have been checked-out prior to science operations. Both Integration and Testing, and Systems Engineering require development.	**2 (IT) 2 (SE)**

Table 3. Preliminary system mass.

Key Subsystem involved in Granular Imager	Mass [Kg]
8 sub-apertures (each D=1 m, and 0.001 Kg/m2)	**0.01**
Laser containment system	**100x6**
Optical bench	**110**
Power Electronics	**20**
Thermal	**20**
Structure	**50**
Communication	**20**
GN&C	**20**
C&DH	**20**
Power Storage	**30**
Propulsion	**30**
Total	**940**

Table 4. Proposed Design Reference Missions for Granular Imager.

	DRM-1	DRM-2	DRM-3
Principal mission	Small Body Remote sensing	Astrophysics	Astrophysics
Secondary mission	Tomographic/topographic radar	Exoplanet detector, coronography	Exoplanet imager, coronography
Orbit	Low-altitude mapping	Sun/Earth-moon L2	Sun/Earth-moon L2
Cloud diameter	10	1-10	1-10
Number of clouds	2 side looking	6-9	>9
Primary diameter, m	N/A	20-100	100-1000
Fill factor	TBD%	< 50 %	< 50%
Wavelength	Microwave (X-W band)	Visible/IR	Visible/IR
Spectral width	Hyperspectral	Broadband	Broadband
Sunlight exposure	No need for shielding	Sun-shade	Sun-shade
FOV	5 deg	1 millirad	<1 millirad
Resolution	1-10 m	<1 milliarcsec	<1 micro arcsec
Average retargeting, deg	No need	10	10
Retargeting time, min	No need	60	60
Targets imaged in 5 yr.	Surface or interior	1e3-1e4	1e3-1e4

Table 5. Driving Requirements and Needed Technologies for Granular Imager

Element	Concept	Driving Requirements	Needed technologies
Detection of habitable worlds	• At L2 • 0.5 to 2 microns • 15-20 m primary • Low fill factor • 2X better than JWST • Sun-shade for thermal loads • Starshade for light suppression	• Microradian and micron pointing stability • Exceptional vibration isolation	• Favorable light-gather vs. fill factor • Star-shade mask coronography • Experiments for stray-light mitigation • Orbital demonstration of formation flying sensing and control • More advanced computational imaging techniques
Imaging of Kuiper Belt Objects	• At L2 • 25 to 50 microns (emissions, temperature) • 0.3-0.9 microns (optical, composition, spectra) • 15-20 m primary • GI inside inflatable • Sun-shade desirable	• KBO tracking • Microradian Pointing and stability • Passive cooling of telescope structure	• Experiments of stray-light mitigation • Orbital demonstration of formation flying sensing and control • More advanced computational imaging techniques

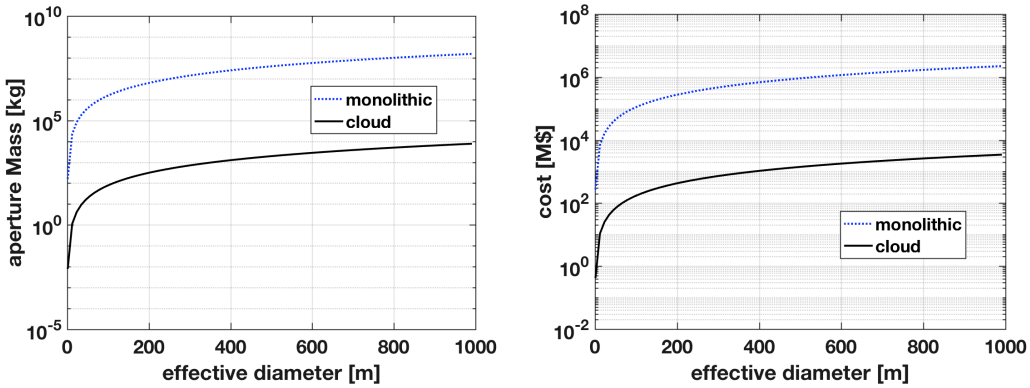

Figure 4. Effective imaging system mass and cost vs. effective diameter, for monolithic and cloud aperture. Cost-benefit analysis is essential to make the cloud aperture more promising compared to the monolithic aperture.

4. POTENTIAL FOR ASTROPHYSICS

The work accomplished by the Exo-C mission concept study [7] is leveraged to quickly derive system requirements to achieve a similar mission. The direct detection of exo-planets requires an imaging system to be able to detect the faint reflected light from the exo-planet while not being blinded by the glare of the parent star the planet orbits. This places stringent requirements on the system to be able to suppress the light from the parent star while leaving the light from the exo-planet intact. For example, as seen from outside our solar system, the brightness of Jupiter at quadrature is given by, B=1/4 (albedo)·(R_J/(5.2 AU))2 ≅ 10^{-9} and detection of an Earth like planet would require starlight suppression on the order of 10-10. Of course it is not enough to just suppress the starlight, you must also maintain starlight suppression stability over the time of a measurement. Otherwise, you signal will be contaminated with stellar light and your contrast will degrade. Exo-planets with stellar contrasts of 10^{-9} will have brightness in the range of V=23-29, with a median of V=27. Therefore depending on the collection area of the imaging system, the integration time may be on the order of multiple days. As a point of reference, the recent Exo-C mission study report quoted integration times of 10 days to spectrally characterize a planet for that system's $3m^2$ collecting area. The spatial field of view (FOV) is the area around a star where planets may be visible to our imaging system. The spatial FOV is defined by two angular measurements: the inner and outer working angles. The inner working angle (IWA) defines how close to a parent star you can see the planet at the required contrasts stated above. The IWA is limited by the imaging system's resolving power and the control bandwidth of an imaging systems starlight suppression system. The outer working angle (OWA) defines how far away from a parent star you can see a planet at or above the required contrast. The OWA is typically limited by the control bandwidth of an imaging system's starlight suppression system. For an ideal perfect imaging system the OWA is limited by the detector's FOV. The EXO-C mission study report quoted a desired IWA of 0.26" at 900nm (0.16" at 550 nm) and a desired OWA of 1.4" at 900nm. After detecting an exo-planet, it will be highly desirable to characterize the spectral features of the exo-planet's signal. Detailed spectral analysis of an exo-planet can be used to determine if a planet has an atmosphere or not. If the exo-planet does have an atmosphere, spectral analysis may enable us to determine the composition of the atmosphere as well. In the previously mentioned Exo-C mission study report, it was determined that to achieve exo-planet characterization a wavelength range of 0.45-1.0μm was desired. This range encompasses several absorption features that are characteristic to molecules needed to support life. They also determined that Exo-planet characterization requires fine spectral sampling to discern features in the spectra. a spectral resolving power of, R~70 was required to achieve exo-planet characterization. Achieving a spectral resolving power of R~70 requires the system to maintain a decent signal to noise (SNR) over spectral elements on the order of SNR ~10.

Based on the above assumptions, an investigation was made of how many photons the granular aperture would collect, and how that photon count would be useful for astronomy. We took the performance parameters of the Hubble detector (see Table 6), and derived an expression for the SNR (signal to noise ratio) and for the exposure time. Some of the parameters used in the equations below are shows in Table 6. For the star Vega, which is magnitude zero and of spectral type A0, $N_0=10^8$ photons/(sec-m2-nm) centered at a wavelength of 550 nanometers in the visible. The photon flux hitting the detector is [31]:

$$S = (N_0 10^{-0.4\,\mathrm{m}})(\pi D^2/4)(1-\varepsilon^2)(\tau)(\Delta\lambda) \tag{2}$$

The background sky-photon flux hitting the detector is [31]:

$$B = (N_0 10^{-0.4\mathrm{m}'})(\phi\phi')(\pi D^2/4)(1-\varepsilon^2)(\tau)(\Delta\lambda) \tag{3}$$

The signal-to-noise ratio can be written as [31]:

$$\mathrm{SNR} = \frac{\kappa S Q t}{\sqrt{(\kappa S + B) Q t + (C_{\mathrm{dark}} t + R^2) \cdot n_{\mathrm{pixel}}}} \tag{4}$$

The exposure time can be written as [31]:

$$t = \frac{1}{2}\left(\frac{(\mathrm{SNR})^2}{\kappa S Q}\right)\left\{\left(1 + \frac{(BQ + C_{\mathrm{dark}}) n_{\mathrm{pixel}}}{\kappa S Q}\right) + \sqrt{\left(1 + \frac{(BQ + C_{\mathrm{dark}}) n_{\mathrm{pixel}}}{\kappa S Q}\right)^2 + \left(\frac{2R}{\mathrm{SNR}}\right)^2 n_{\mathrm{pixel}}}\right\} \tag{5}$$

Figure 6 shows the SNR vs. apparent magnitude for 50% and 100% fill factor. Figure 7 shows the exposure time vs. apparent magnitude for 50% and 100% fill factor. These plots indicate that, even for low fill factor, the performance of the granular cloud as a photon bucket is still satisfactory, and can be used as a science instrument of performance comparable to HST (assuming all other detector parameters remain the same).

Table 6. Observation dependent parameters, based on Hubble detector model (taken from [31]).

Grain diameter	100 microns
Cloud encircled diameter, D*fillFactor	1 m
Star magnitude, m	M
Detector area projected onto sky	0.1 x 0.1 micron^2
Instrument filter bandpass, $\Delta\lambda$	100 nm
Secondary mirror optical blockage, ε	0.33
System transmittance, τ	0.324
fraction of 550nm transmitted light to detector, κ	0.8
quantum efficiency within filter BW, Q	0.8
Dark noise, C_{dark}	0.003 electrons/s/pixel
Readout noise	5 electrons-rms/pixel

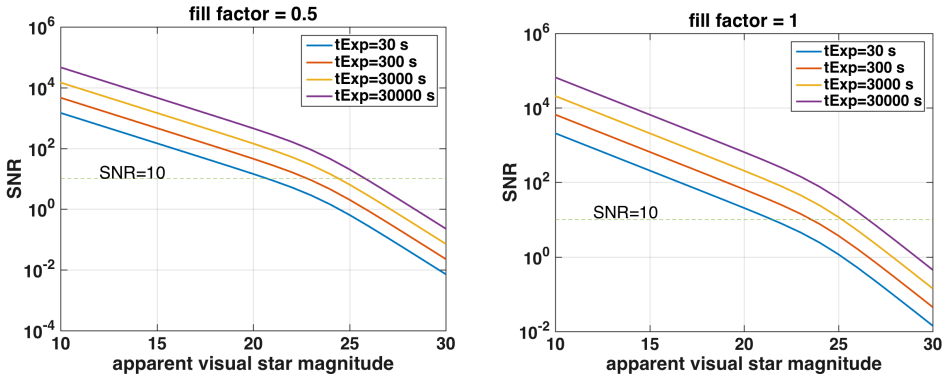

Figure 5. SNR vs. apparent magnitude for 50% and 100% fill factor.

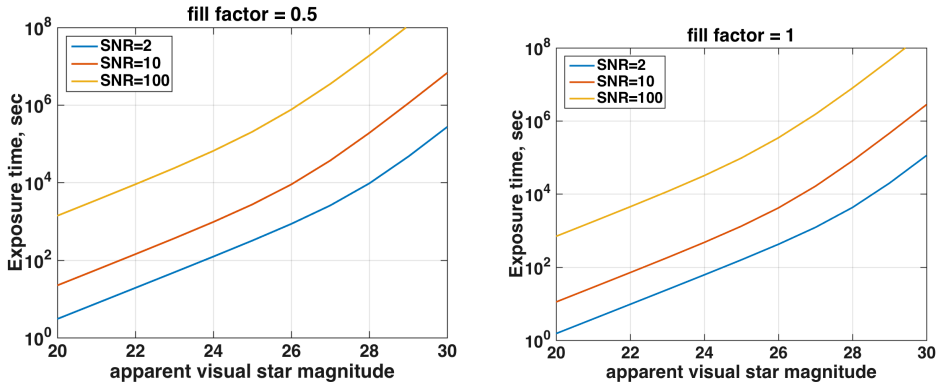

Figure 6. Exposure time vs. apparent magnitude for 50% and 100% fill factor.

5. SENSING AND CONTROL

In the following, we outline the dynamics and control architecture for the GI imager. Figure 8 describes the overall control architecture for the system model. It starts in the upper left corner with the GI model, which would include a model of the system dynamics. This dynamics engine computes the dynamic response of the telescope system in formation, including the primary aperture. It receives model updates as data from the planned laboratory experiments becomes available. The control involved at this level includes the control of the granular sub-aperture elements, and the control of the entire aperture formed by the sub-apertures. From the dynamic state of the random patch elements, a complex electromagnetic pupil function is computed, from which the optical figure and pupil can be determined. The next stage of control involves feedback on the relative position and orientation of the separate spacecraft imaging system (primary and secondary) to keep the elements in formation. The spacecraft has its own thrusters and reaction wheels to maintain precision optical alignment using a laser metrology truss. A STOPC (Structural, Thermal, Optical, Control) integrated model is the basis of the wavefront sensing and control system. Drivers to the STOP model include thermal variations based on the trajectory of the system relative to the Sun and other thermal sources. The STOP model has two main control systems, one for LOS correction and an adaptive optics control system that uses a Shack-Hartmann sensor to control a deformable mirror. Combining information from multiple STOP models (one for each granular patch element), a time-varying PSF (Point Spread Function) of the optical system is computed. An IPO (In-focus PSF Optimizer) is another WFS&C algorithm developed at JPL for segmented optical systems. This algorithm could be used to drive the optical delay lines to maintain the relative phase of each granular patch and would also provide feedback information to the LOS control to maintain high-level system pointing. Finally, the time-varying PSF is convolved with an image (or "scene"). Speckle imaging and multiframe blind deconvolution algorithms could be used to "clean up" the imagery to get an accurate estimate of the original scene. Table 7 summarizes the different sensing and actuation techniques that would be used to enable the GI image stabilization.

Table 7. Sensing and actuation methodologies.

Element	Comments
WFSC Sensing	Shack-Hartmann wavefront sensor
WFSC Actuation	Fast Steering Mirror (FSM): Provides tip/tilt (jitter) correction. Deformable Mirror (DM): Provides Mid-Spatial Frequency (figure) correction. Optical Delay Line: Provides patch-to-patch coarse alignment (phasing).
FF Sensing	RF (coarse), Laser (Fine) metrology
FF Actuation	MEMS microthrusters, Reaction wheel, Disturbance isolation
Confinement Sensing	LIDAR Camera
Confinement Actuation	Electrodynamic confinement

Next, we outline the modeling and control architecture for control of the GI array, shown in Figure 8. We adopt a previous approach proposed for a membrane mirror telescope. We divide this approach into a static loop and a dynamic loop. The static solution for the granular mirror displacement is used to optimize the actuation so that the resulting aberrations are gone. Therefore, an iterative process is required to optimally distribute the electromagnetic confinement loads at the boundary. Mirror surface deformations are then computed at each time step given the external perturbation sources and the actuator inputs. With these mirror surface deformations, the deformed aperture shape can be synthesized. The coefficients of the Zernike polynomials are then identified, and the corresponding confinement/shaping voltages are then computed. These voltages are compared with the static voltages required to attain the ideal spherical surface, and a corrective control action is requested with an additional voltage correction. This is shown in Figure 8.

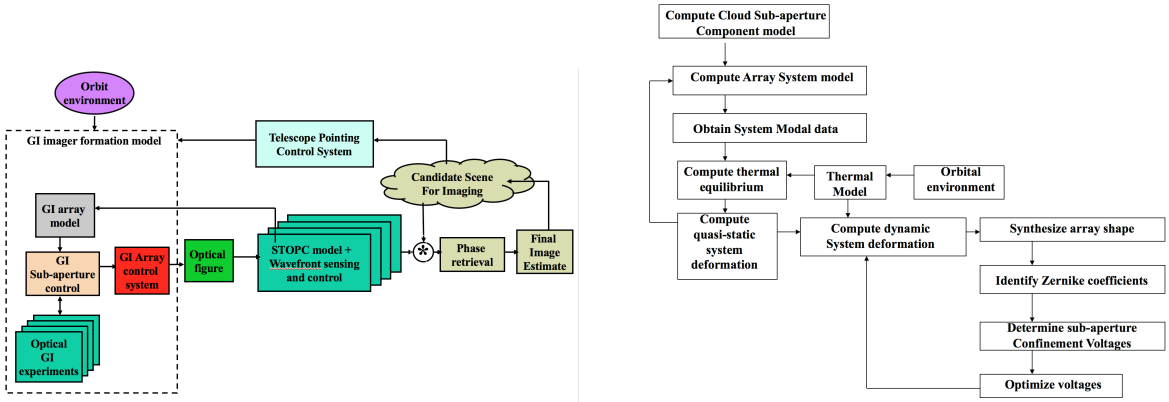

Figure 7. (Left) Integrated Modeling for Control of the Granular Imager. (Right) Modeling and control architecture requiring design iteration.

This section details a control system that may be used in conjunction with the electrodynamic trapping system to correct the wave-fronts so that the granular imager will generate high resolution image that fully realize the potential of larger aperture sizes. The challenge of a wavefront control system for a granular imager is to correct for the scattered speckle field when the effective surface roughness of the granular media is on the order of microns. It is unlikely that a single deformable optic will have both the range and control accuracy to correct for such roughness. Therefore, we opted for a staged control architecture. The wavefront control process follows the following steps: A) **Granular Cloud Shaping** – Grains are trapped in an optical trap, where they are shaped into a conic section; B) **Sub Aperture Coarse Alignment** – The trapped grains may be broken into regions or sub-apertures. Correcting for coarse misalignments between sub-apertures, corrects the low spatial frequency surface roughness of our granular imager, thereby making the PSF of the granular imager more compact. C) **Figure Control** – Now that each sub-aperture is controlled globally with respect to each other, we can control the figure of each sub-aperture. D) **Computational Imaging**. A combination of PSF deconvolution techniques and computational imaging will be used to compensate for less-than-ideal imaging as a result of the granular nature of the primary mirror.

In the following, we outline the modeling and control architecture we envision to realize a closed loop control system that makes use of the granular primary shape estimation scheme. We divide this control architecture into an acquisition step, a trapping step, a rigidification step, a shaping step, a static step, and a dynamic step, as summarized in Figure 9.

Acquisition Step: The acquisition step begins when the cloud, previously ejected from a canister, is detected and its position and attitude are acquired by a lidar system.

Trapping Step: Once acquired, the trapping step involves the capture and stabilization of the cloud inside a capture volume. The capture volume is defined as the volume in space where a granular patch needs to be placed as an element of a sparse aperture system. The cloud is trapped by an external trapping mechanism of an electrostatic or magnetostatic

type. The external confinement mechanism is based on the principle of the Optical Tweezer. It relies on a combination of the scattering and gradient optical force on the grains to trap them into equilibrium states.

Rigidification step: The rigidification step assumes that the trapped cloud is first driven to crystallization inside the capture volume by the external confinement mechanism. Once rigidified inside the capture volume, the cloud takes the form of a thin compressed carpet, and is kept stably in that form. Low frequency oscillations can and will occur, due to long period perturbations such as gravitational harmonics, but essentially, the cloud behaves like a rigid body inside the capture volume.

Shaping step: In the shaping step, the rigidified granular layer is now gradually shaped into a spherical surface by differentially actuating the confinement mechanism to produce the resulting shape. It involves sensing of the cloud's position and three-dimensional shape via a lidar system, and actuating the cloud by a modulated electric field distribution from the confining electrodes.

Static step: Once shaped, the cloud behaves like an equivalent rigid reflector. Once a model is developed of a shaped granular layer, the capability is available to model the entire spherical mirror surface undergoing static deformations. The static solution for the mirror displacement is used to optimize the electrode potential distributions so that the resulting aberrations are gone. Therefore, an iterative process is required to optimally distribute the electrode potentials. To do this, we propose a quasi-static modal control approach for the granular mirror shape control. Then, an algorithm that computes the required boundary actuation will adjust the coefficients in these series in order to establish the desired spherical mirror shape. Our approach is to define a desired shape for the mirror, and then to describe the deviation from this shape in terms of Zernike series, and to adjust the Zernike coefficients with a control actuation. At the Sun-Earth L2 point, the large mirror will be exposed to disturbance forces, which vary extremely slowly, such as solar pressure. Therefore, we can treat the shape control of the large mirror as finding the control forces to correct the static deformations at a given time. The dynamics of the mirror are ignored in this approach, so the approach is static in nature. But, since this correction is done frequently, and the external control actuation can be applied very rapidly, this is a reasonable simplification.

Dynamic step: Once this initial static step is completed, the system dynamics can be computed, and the system modal data evaluated. An integrated modeling approach previously considered for high-precision space telescopes is followed in the development of the system model for control design [21]. The granular aperture dynamic model is a model of the system in modal space, obtained from the mass and stiffness (M,K) set. The solution is based on a continuous to discrete transformation in 2nd order form $\ddot{\eta}_k + 2\Sigma\Lambda\dot{\eta}_k + \Lambda^2\eta_k = \Phi^T f_k$ where Σ, Λ are diagonal (n x n) and the modal displacement η_k is (n x 1), and n is the number of retained modes. From the global stiffness matrix of the cloud, we can derive the generalized compliance, i.e. the influence functions. Influence functions are the mappings $\frac{\partial u_{Ki}}{\partial f_{Nj}}$, where u_{Ki} is the displacement at location K in the i-th direction, and f_{Nj} is the control action at location N in the j-th direction.

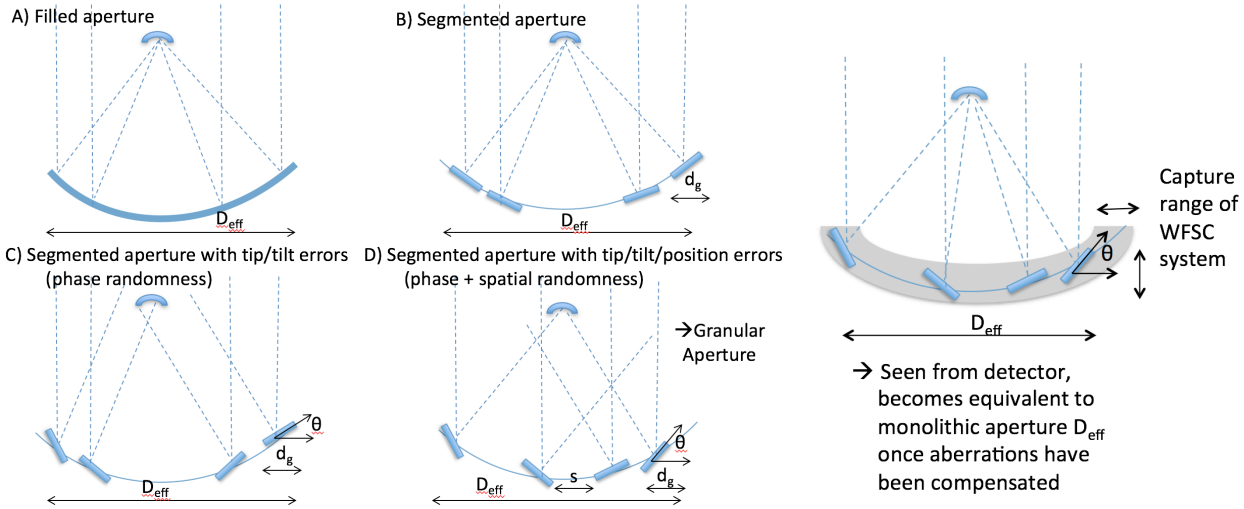

Figure 8. (Left) Comparison between monolithic, segmented, segmented with tip/tilt errors, and segmented with til/tilt and geometric disorder. (Right) Confined granular medium would operate as an equivalent monolithic aperture if range of particle motion is constrained to stay within the capture range of the WFSC system.

6. INTERACTION OF GRANULAR MEDIUM WITH INCIDENT WAVEFRONT

We conducted experiments and simulation of the optical response of a granular lens. In all cases, the optical response, measured by the Modulation Transfer Function (MTF), of large numbers of hexagonal reflectors was closely comparable to that of a spherical mirror. We conducted the analyses further by evaluating the sensitivity to fill factor and grain shape, and we found a marked sensitivity to fill factor and no sensitivity to grain shape. However, we found that at fill factors as low as 30%, the reflection from a granular lens is still excellent. In fact, we replaced the monolithic primary of an existing integrated model of an optical system (W-First Coronagraph) with a granular lens, and we found that the granular lens that can be useful for exoplanet detection provides excellent contrast levels.

6.1 Sensitivity Studies

By varying 11 error parameters of the MCB/HLC optical system (AFTA), we wanted to verify that we could get a good agreement between the measured and the simulated closed-loop mean contrast, and determine the degree of accuracy of the 11 error parameters chosen by comparing the measured and the simulated open-loop contrast curves, changing the value of one error term at a time. This exercise validated the results obtained last year just before the midterm review, and give us confidence of the advantages of the random spatial disorder and low fill factor to synthesize an image with sufficient photon count. Figure 10 shows the Point Spread Function and Modulation Transfer Function for different grain numbers. Figure 11 shows the pupil amplitude, the point spread function, and the contrast metric for 2 mm particles with 20% fill factor. Figure 12 shows the sensitivity of the Modulation (MTF) to fill factor, and the details of the generation of an elliptical random mask. Figure 13 shows the result of the MTF of six sets of random masks compared to ideal monolithic aperture, and the Strehl ratio vs. fill factor. The Modulation Transfer Functions (MTF) of various random masks were evaluated numerically, including the effect of the grain shape. Figure 14 shows a 5x5 pixel random mask with rounded edges, and the effect of grain shape and pixel size on system MTF for a 40% fill factor, indicating that the shape of the grains does not have a pronounced effect on the optical response.

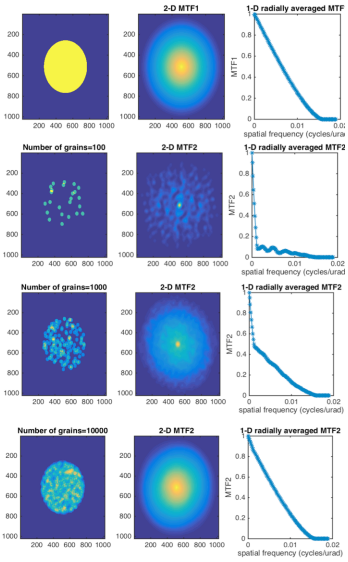

Figure 9. Point Spread Function and Modulation Transfer Function for different grain numbers.

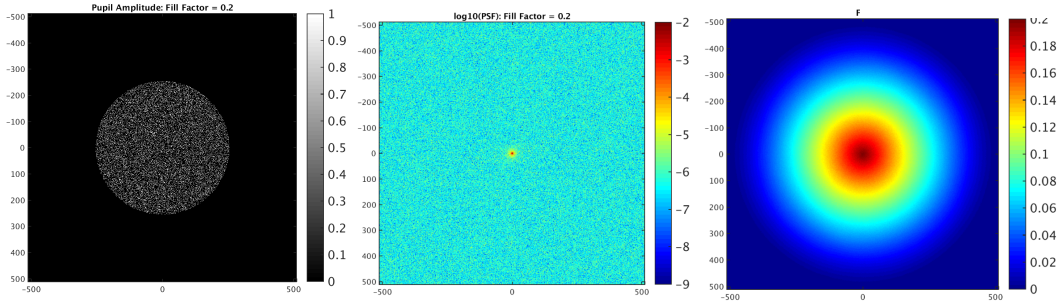

Figure 10. (Left) Pupil amplitude, (Center) Point spread function, (Right) contrast metric for 20% fill factor.

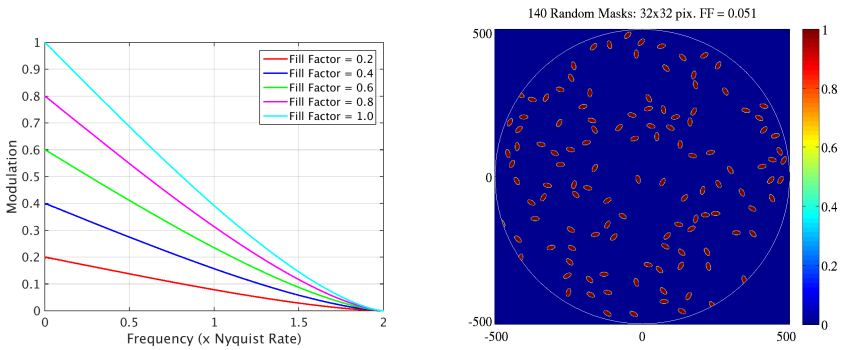

Figure 11. (Left) Sensitivity of Modulation (MTF) to fill factor. (Right) Pupil partially filled with random masks.

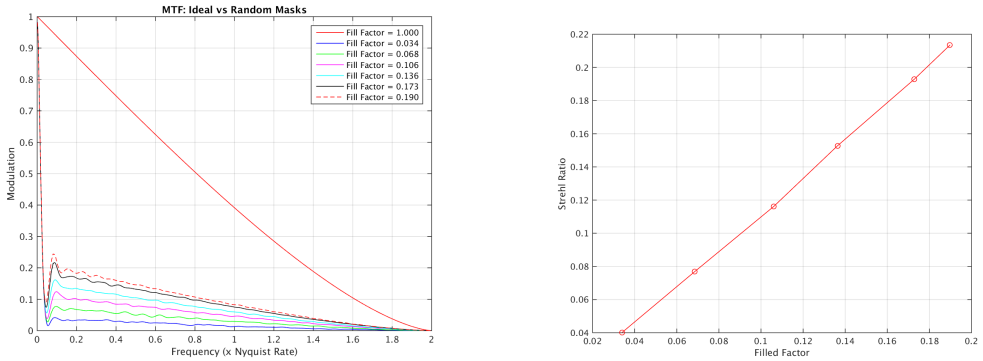

Figure 12. (Left) MTF of six sets of random masks compared to ideal monolithic aperture. (Right) Strehl ratio vs. fill factor.

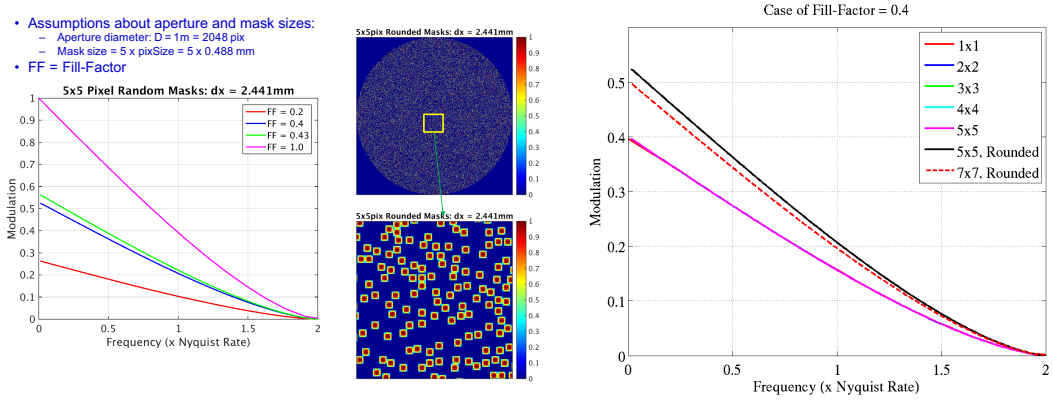

Figure 13. (Left) 5x5 pixel random mask with rounded edges. (Right) Effect of grain shape and pixel size on system MTF.

6.2 Preliminary Experiment with Hexagonal Reflectors

Several implementations of the Granular Imager were examined experimentally. Figure 15 shows a few of the granular lenses that were tested. Figure 16 shows two sets of images generated with the hexagonal reflectors and captured at different reflectors-camera distances. In this experiment, the camera was mounted on a free-standing post was moved by hand from a position to the next. If we image a collimated light using an ideal lens, we obtain a PSF and MTF shown in Fig. 17. However, in this experiment, we first imaged a collimated beam using a spherical mirror (D = 25mm, beam diameter ~ 20mm). Because of the limitations in hardware, space and time, we had to operate the spherical mirror at a large tilt angle (angle of incidence of ~ 20 degrees). This introduced severe aberration in the measured PSF image, and also resulted in a poor MTF characteristics (see Fig. 17, two left plots). Next, we sandwiched small, hexagonal reflectors between a concave and a convex lens having the same radius of curvature, as shown in Fig. 18, bottom left. By reflecting a collimated beam from that reflecting sub-assembly, we produced an image, as shown in the top-right plot of Fig. 17. We also calculated its MTF. Figure 18 compares the 1-D MTF curves of an ideal PSF, the image obtained with the spherical mirror, and the image obtained with the hexagonal reflectors. As we can see, the MTF of the hexagonal reflectors is very much comparable to that of the spherical mirror.

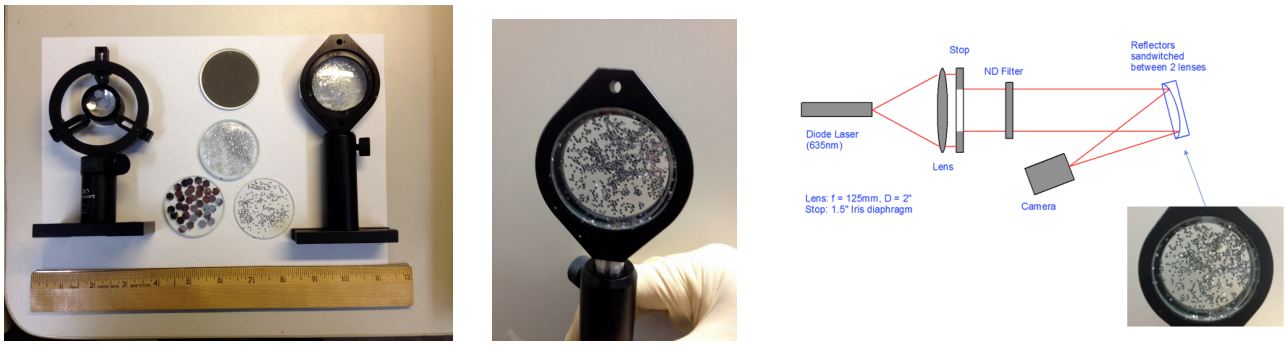

Figure 14. (Left) Different granular lenses used in the experiments. (Right) Schematic diagram of experimental setup to measure the Modulation Transfer Function of the Granular Imager.

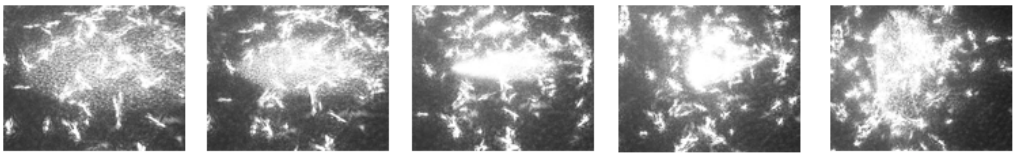

Figure 15. One set of images generated with the hexagonal reflectors and captured at different reflectors-camera distances.

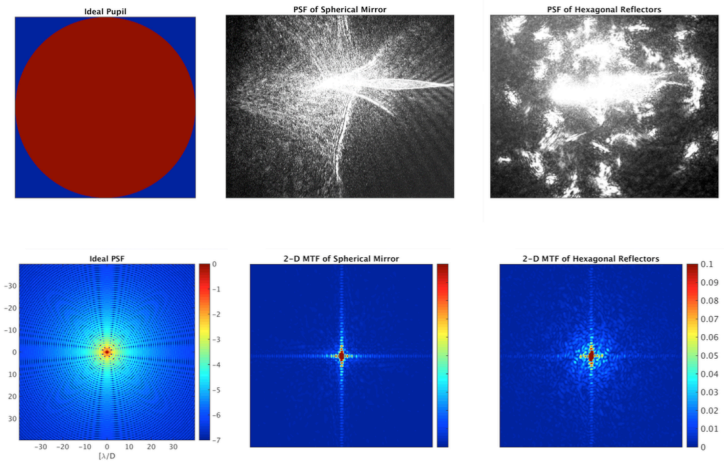

Figure 16. Comparison of MTF of ideal lens, spherical mirror, and granular hexagonal mirror.

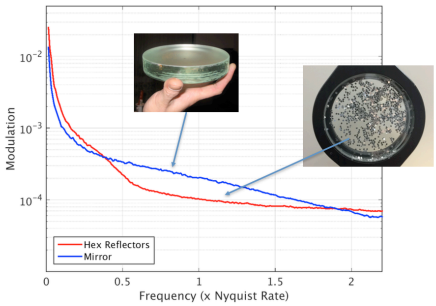

Figure 17. Comparison of experimental modulation transfer function (MTF) of continuous mirror with granular mirror with hexagonal elements.

6.3 Granular medium confinement

The details of the mechanics of trapping and confinement are discussed in a companion paper [29]. In the experiment, we used an ion trap to test different configurations of levitated granular media. The ion trap was procured from Newtonian Labs, Inc., from Pasadena, CA. The ion trap allowed us to conduct a broad range of qualitative and quantitative ion trapping experiments. Components of the ion trap include: a) Three plug-in ion traps (The Ring Trap, The Linear Trap, The Single Particle Trap); b) A High-Definition still+video camera, including live-view HDMI video; c) Macro and micro optics for video viewing of trapped particles; d) A steerable green laser for particle illumination, e) a HDMI TV screen. Figure 19 shows the ion trap set-up. With this set-up, we have successfully stably levitated single particles and aggregates of multiple particles inside an ion trap. While the ion trap technique is very promising for the Granular Imager, we were able to levitate grains with a q/m ration comparable to that of 10-100 micron grains (mass of the order of the nanogram, and charges of the order of 10^5 electron charges). We were successful in stably trapping and levitating single particles and aggregates of particles in air. Once levitated, these clouds of grains displayed a remarkable regularity and stability over time, typical of Coulomb crystal behavior. This was expected. The particles used were in the 30-100 micron diameter range. The charge to mass ratio of the ion trap was tailored for optimal levitation of nanogram particles, so larger size grains could not be contained due to their excessive mass. Consequently, further work will require ion traps with larger electrostatic potentials, or particles with larger electron charge to compensate for the larger mass. Figure 19 also shows one of the stable trapped cloud inside the trap.

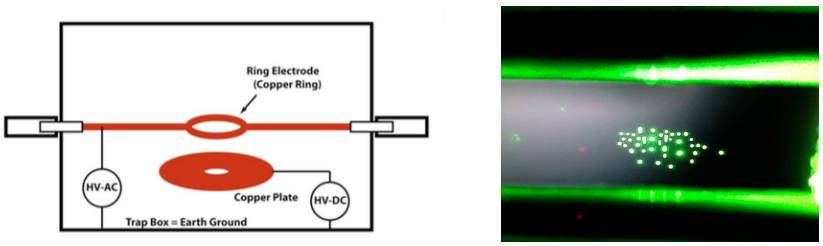

Figure 18. (Left) Schematics of ring trap From Newtonian Labs. (Right) Photo of levitated clouds of silver coated hollow glass microspheres (100 micron diameter).

7. CONCLUSIONS

Our objective has been to experimentally and numerically investigate how to optically manipulate and maintain the shape of an orbiting cloud of dust-like matter so that it can function as an adaptable ultra-lightweight surface. Our solution is based on the aperture being an engineered granular medium, instead of a conventional monolithic aperture. This allows building of apertures at a reduced cost, enables extremely fault-tolerant apertures that cannot otherwise be made, and directly enables classes of missions for exoplanet detection based on Fourier spectroscopy with tight angular resolution and innovative radar systems for remote sensing. We have examined the advanced feasibility of a crosscutting concept that contributes new technological approaches for space imaging systems, autonomous systems, and space applications of optical manipulation. We presented some ideas regarding the optics and imaging aspects of a granular spacecraft. Granular spacecraft are complex systems composed of a spatially disordered distribution of a large number of elements, for instance a cloud of grains in orbit. An example of application is a spaceborne observatory for exoplanet imaging, where the primary aperture is a cloud instead of a monolithic aperture. The application considered so far was a reflective imaging system for astrophysics, but many unexplored applications of granular spacecraft are yet to be discovered. The results of the numerical tests indicate that it is possible, with structural arrangements of rings and plates at different levels of electrostatic potential, to stably confine one or more charged particles, when driven by voltages that can be modulated in time and space. We conducted experiments and simulation of the optical response of a granular lens. In all cases, the optical response, measured by the Modulation Transfer Function, of the hexagonal reflectors was

closely comparable to that of the spherical mirror. We conducted the analyses further by evaluating the sensitivity to fill factor and grain shape, and we found a marked sensitivity to fill factor and no sensitivity to grain shape. However, we found that at fill factors as low as 30%, the reflection from a granular lens is still excellent. In fact, we replaced the monolithic primary of an existing integrated model of an optical system (W-First Coronagraph) with a granular lens, and we found that excellent contrast levels are provided by the granular lens that can be useful for exoplanet detection. We have successfully stably levitated single particles and aggregates of multiple particles inside an ion trap. While the ion trap technique is very promising for the Granular Imager, we were able to levitate grains with a q/m ration comparable to that of 10-100 micron grains (mass of the order of the nanogram, and charges of the order of 105 electron charges). We were successful in stably trapping and levitating single particles and aggregates of particles in air. Once levitated, these clouds of grains displayed a remarkable regularity and stability over time, typical of Coulomb crystal behavior. Further work will require ion traps with larger electrostatic potentials, or particles with larger electron charge to compensate for the larger mass.

Near-term proof-of-concept space demonstrations might be possible in a decade, but laboratory-scale tests on Earth are possible much sooner. This concept is technically feasible given that it is drawn from real-world examples of dust/droplet systems like rainbows. Our solution would completely rewrite our approach to ultra-large space-based telescopes for potential NASA origins, Earth sensing, and potentially also for military applications. All the foundations of the concept are solidly based on established physical laws. The challenge is extending what has been proven in small lenses in an Earth environment to a space environment under various forces and the means to predict and control those forces for a long time to get the full benefit of the concept. There is no guarantee that this breakthrough innovative system will meet the configuration or design of a large aperture system at various parts of the electromagnetic spectrum, but even if a few of those areas are or can be identified, the benefit to NASA and national security will be immense.

ACKNOWLEDGMENTS

This research was carried out at the Jet Propulsion Laboratory, California Institute of Technology, under a contract with the National Aeronautics and Space Administration funded by the NASA Innovative Advanced Concepts (NIAC) program under contract 14-14NIAC-II-0008 (Orbiting Rainbows, Phase II). The authors are grateful to Prof. Grover Swartzlander of Rochester Institute of Technology for useful discussions. The cost information contained in this document is of a budgetary and planning nature and is intended for informational purposes only. It does not constitute a commitment on the part of JPL and/or Caltech.

REFERENCES

[1] Andersen, T., and Enmark, A.: Integrated Modeling of Telescopes, Springer Astrophysics and Space Science Library, vol. 377, 2011.
[2] Ashkin, A., Optical trapping and manipulation of neutral particles using lasers, Proc. Natl. Acad. Sci. 94, 4853-4860 (1997)].
[3] Bekey, I.: An extremely large, yet ultra-lightweight space telescope and array, NIAC Phase I report, 1999.
[4] Born, M., and Wolf, E.: Principles of Optics, 2nd edition, Pergamon Press, 1964, pp. 400
[5] Brady, D.J., Hagen, N.: Multiscale lens design, Opt. Express 17, 10659-10674, 2009
[6] Cubesat NRC report, http://www.nap.edu/catalog/23503/achieving-science-with-cubesats-thinking-inside-the-box
[7] Science Plan for NASA's Science Mission Directorate, 2007-2016.
[8] Choi et al: Overcoming the Diffraction Limit Using Multiple Light Scattering in a Highly Disordered Medium, PRL 107, 023902, 2011.
[9] Davis, E.J., and Schweiger, G.: The Airborne Microparticle, Springer, 2012.
[10] Dienerowitz, M.: Plasmonic Effects upon Optical Trapping of Metal Nanoparticles, PhD Thesis University of St. Andrews, U.K., 2010.
[11] Fuchs, N.A.: The Mechanics of Aerosols, Dover Publications, 1989.

[12] Grzegorczyk, T.M. et al.: Optical Mirror from Laser-Trapped Mesoscopic Particles, Physical Review Letters, 112, 023902 (2014).
[13] Hyde, R.A., "Eyeglass: Large Aperture, Lightweight Space Optics", LLNL Report UCRL-ID-151390 (2003).
[14] Kokhanovsky, A. A.: Cloud Optics, Springer, 2006.
[15] Labeyrie, A.: Standing Wave and Pellicle: A Possible Approach to Very Large Space Telescopes, Astronomy and Astrophysics, 77, L1-L2, 1979.
[16] Labeyrie, A., M. Guillon and J.-M. Fournier: Optics of "Laser Trapped Mirrors" for large telescopes and hypertelescopes in space, SPIE Proc. 5899, 2005.
[17] Labeyrie, A.: Attainment of diffraction limited resolution in large telescopes by Fourier analysing speckle patterns in star images. Astron. Astrophys, 6(1):85–87, 1970.
[18] Major, F.G., V.N. Gheorghe, and G. Werth: Charged Particle Traps. Physics and Techniques of Charged Particle Field Confinement, Springer, 2005.
[19] McCormack, et al., Laser Trapping of Mirrors in Space, NIAC Phase I report, 2006.
[20] Mettler E., Breckenridge W.G., and Quadrelli M.B.: Large Aperture Telescopes in Formation: Modeling, Metrology, and Control, The Journal of the Astronautical Sciences, vol. 53, no.5 October-December 2005, pp.391-412.
[21] Mosier, G., M., Fermiano, K. Ha, P. Bely, R. Burg, D. Redding, A. Kissil, J. Rackozy, L. Craig: "Fine Pointing and Control for a Next generation Space Telescope, Part of the SPIE Conference on Space Telescopes and Instruments, V, Kona, Hawaii. March1998.
[22] Palmer, A.J.: Nonlinear Optics in Aerosols, Optics Letters, vol. 5, no. 2, February 1980
[23] Palmer, A.J.: Radiation-induced Orientation of Atmospheric Aerosols, J. OP. Soc. America A, vol. 8, no. 2, February 1991.
[24] Peng, X., Ruane, G., Swartzlander, G., and Quadrelli, B.M.: Randomized Apertures: high resolution imaging in far field, submitted to Optics Express, 2017.
[25] https://www.nasa.gov/directorates/spacetech/niac/2012_phase_I_fellows_quadrelli.html
[26] Quadrelli, M., Basinger, S., Swartzlander, G.: Dynamics and Control of a Disordered System in Space, AIAA SPACE 2013 Conference, San Diego, Ca, Sept. 2013.
[27] Quadrelli, B.M., Basinger, S., Swartzlander, G., Darmin Arumugam, D.: Dynamics and Control of Granular Imaging Systems (AIAA 2015-4484), AIAA SPACE 2015 Conference and Exposition, 2015, 10.2514/6.2015-4484.
[28] Basinger, S.,Palacios, D. , Quadrelli, B.M., Swartzlander, G.: Optics of a granular imaging system (i.e. "orbiting rainbows"), Proceedings SPIE paper 9602-13, SPIE Optics/Photonics Conference, UV/Optical/IR Space Telescopes and Instruments: Innovative Technologies and Concepts VII, San Diego, CA, 9-13 August 2015.
[29] Quadrelli, B.M., Ius, P., Lanzoni, L.: Modeling and Simulation of Trapping Mechanisms of Granular Media In Space, presented at the AIAA SPACE 2016 Conference, Long Beach, CA, Sept. 2016.
[30] Scharmer, G.B., Lofdahl, M.G., van Werkhoven, T.I.M. de la Cruz Rodriguex, J., "High-order aberration compensation with multi-frame blind deconvolution and phase diversity image restoration techniques", A&A Vol. 521, A68 (2010).
[31] Schroeder, D.: Astronomical Optics, Academic Press, 2000.
[32] Shvedov, V., Rode, A., Izdebskaya, Y., Desyatnikov, A., Krolikowski, W., and Kivshar, Y.: Giant Optical Manipulation, Phys. Rev. Lett. 105, 118103 (2010).
[33] Simpson, S. H., Hanna, S., Peterson, T. J., and Swartzlander, G. A. Jr. Optical lift from dielectric semicylinders, Optics Letters 37, 4038-4040 (2012)].
[34] Stahl, H. P., Survey of Cost Models for Space Telescopes, Optical Engineering, Vol. 49, No. 5, May 2010.
[35] Summers, M. D.: Optical Micromanipulation of Aerosols, PhD Thesis University of St. Andrews, U.K., 2009.
[36] Swartzlander G. A., Peterson, T. J., Artusio-Glimpse A. B., Raisanen A. D.: Stable optical lift. Nature Photonics, Nature Photonics 5, pp.48–51, 2011.
[37] Tyson, R., Principles of Adaptive Optics, Academic Press, 1997.
[38] Vellkhoop et al, Exploiting disorder for perfect focusing, arXiv:0910.0873v1.
[39] Yavuz, D.: Frequency and Focal Region Properties of Random Sparse Arrays, IEEE Transactions on Antennas and Propagation, vol. AP-32, no. 5, May 1964.
[40] Zhao, F.: Development of high-precision laser heterodyne metrology gauges, SPIE Proc. Vol. 5634, 14 Feb. 2005, Advanced Sensor Systems and Applications II, Yun-Jiang Rao; Osuk Y. Kwon; Gang-Ding Peng, Editors, pp.247-259.